Contribution from the Instituto de Ciencia de Materiales de Aragón, Facultad de Ciencias, Universidad de Zaragoza-CSIC, 50009 Zaragoza, Spain, and Laboratoire de Physique des Solids, Bâtiment 510, Université Paris-Sud, 91405 Orsay Cedex, France

Rectangular and Hexagonal Columnar Mesophases in Dinuclear Rhodium(II) (Alkyloxy)benzoate Complexes

Joaquin Barberá,[†,‡] Miguel A. Esteruelas,[†] Anne Marie Levelut,[‡] Luis A. Oro,*[,†] Jose L. Serrano,[†] and Eduardo Sola[†]

Received June 25, 1991

The complexes $[Rh_2(\mu\text{-}O_2CC_6H_4\text{-}4\text{-}OC_nH_{2n+1})_4]$ (n = 8–14), $[Rh_2(\mu\text{-}O_2CC_6H_3\text{-}3,4\text{-}(OC_{10}H_{21})_2)_4]$, and $[Rh_2(\mu\text{-}O_2CC_6H_2\text{-}3,4,5\text{-}(OC_{10}H_{21})_3)_4]$ were prepared by the reaction of $[Rh_2(\mu\text{-}O_2CCH_3)_4]$ with the corresponding (alkyloxy)benzoic acids. The adducts $[Rh_2(\mu\text{-}O_2CC_6H_4\text{-}4\text{-}OC_{10}H_{21})_4(CO)_2]$ and $[Rh_2(\mu\text{-}O_2CC_6H_4\text{-}4\text{-}OC_8H_{17})_4(N_2C_4H_4)]_n$ were obtained by treatment with CO and pyrazine, respectively. Cyclic voltammograms of $[Rh_2(\mu\text{-}O_2CC_6H_4\text{-}4\text{-}OC_nH_{2n+1})_4]$ complexes show reversible one-electron oxidation processes. The thermal behavior of the complexes was investigated by optical microscopy and DSC, and the structures of the mesophases and solid phases obtained were determined by X-ray diffraction. The complexes $[Rh_2(\mu\text{-}O_2CC_6H_4\text{-}4\text{-}OC_nH_{2n+1})_4]$ (n = 10–14) display two orthorhombic crystal phases at room temperature (space groups *Pmmm* and *Pbmn*) and a columnar mesophase of rectangular (orthorhombic) symmetry (space group *Cmmm*). For the n = 10 homologue the cell parameters are as follows: a = 23.50 Å, b = 13.19 Å, c = 4.82 Å, (Z = 1), in the *Pmmm* phase; a = 49.30 Å, b = 12.96 Å, c = 4.86 Å (Z = 2), in the *Pbmn* phase; a = 55.05 Å, b = 13.06 Å, c = 4.86 Å (Z = 2), in the *Cmmm* mesophase. The eight-chained complex shows two columnar phases, one rectangular at room temperature (likely *Cmmm*; a = 45.7 Å, b = 30.01 Å) and a hexagonal one above 138 °C (*P6/mmm*; a = 29.1 Å). The twelve-chained derivative exhibits a 3D monoclinic phase at room temperature (space group *P2/m*; cell parameters a = 33.28 Å, b = 20.38 Å, c = 10.10 Å, γ = 113.3°, Z = 1) and a hexagonal columnar mesophase at higher temperatures (*P6/mmm*; a = 26.6 Å).

Introduction

Liquid crystalline complexes of transition metals have received increasing attention in recent years, owing to the possibilities offered by the metal for both the design[1] and practical application[2] of these materials. In particular, complexes that show columnar mesophases are specially interesting due to their potential ferromagnetic or electron transport properties.[3-5]

Two years ago we reported the first family of iridium liquid-crystal complexes. These complexes, *cis*-[IrCl(CO)L] (L = $NC_5H_4CH{=}NC_6H_4R$), were formed by the complexation of the non-mesogenic organic ligands L to the metal.[6] In subsequent papers, we presented the synthesis of the related mesogenic rhodium derivatives *cis*-[RhCl(CO)L][7] and four new series of ionic silver complexes for which thermotropic liquid-crystal properties were observed.[8] Continuing with our work in this field, and as part of a general study of new liquid crystals of iridium-, rhodium-, and silver-containing nitrogen- and oxygen-donor ligands,[9] we can now report the synthesis and characterization of new mesogenic rhodium(II) (alkyloxy)benzoate complexes, which show columnar mesophases where the symmetry of the resulting lattice is rectangular or hexagonal, depending on the number of chains of the benzoate ligands.

For the columnar mesophases displayed by metallomesogens, the symmetry of the lattice is generally hexagonal, as has been found in metallic complexes containing β-diketonates,[10] porphyrines,[5] and phthalocyanines[3,4] as ligands. Alkanoate complexes of Cr, Mo,[11] Ru,[12] Rh,[13] and Cu[14] also show this type of mesophase. Examples of mesogenic metal complexes displaying non-hexagonal columnar mesophases are very rare. The existence of rectangular columnar mesophases has been suggested in order to explain the occurrence of columnar polymorphism in some macrocyclic Cu(II) complexes,[15] and to the best of our knowledge, only the disordered rectangular columnar mesophase of the complex (octakis(dodecyl)tetrapyrazinoporphyrazino)copper(II) has been characterized by X-ray diffraction.[16]

Results

Synthesis and Characterization. Preparation of the complexes $[Rh_2(\mu\text{-}O_2CC_6H_4\text{-}4\text{-}OC_nH_{2n+1})_4]$ (n = 8 (**1**), 9 (**2**), 10 (**3**), 11 (**4**), 12 (**5**), 13 (**6**), 14 (**7**)) involves the exchange of the bridging ligands of the $[Rh_2(\mu\text{-}O_2CCH_3)_4]$ complex, by heating this dimer in a melt of the corresponding 4-(alkyloxy)benzoic acid. Complexes **1**–**7** were obtained as green solids in yields of about 60%. The IR spectra (Nujol) of these complexes show the absorptions due to

Table I. Half-Wave Oxidation Potentials (V) and ΔE_p[a] (in Parentheses (mV)) for $[Rh_2(\mu\text{-}O_2CC_6H_4\text{-}4\text{-}OC_nH_{2n+1})_4]$ Complexes

complex	n	CH_2ClCH_2Cl	THF	CH_2ClCH_2Cl/CH_3CN[b]
2	9	1.12 (157)	1.13 (204)	
3	10	1.16 (163)	1.11 (177)	1.08 (90)
4	11	1.12 (160)	1.13 (225)	1.08 (90)
5	12	1.15 (191)	1.12 (194)	1.08 (122)
6	13		1.12 (213)	
7	14		1.12 (167)	

[a] Sweep rate 50 mV s^{-1}. [b] Relation 10/1.

(1) (a) Adams, H.; Bailey, N. A.; Dhillon, R.; Dunmur, D. A.; Hunt, S. E.; Lalinde, E.; Maggs, A.; Orr, R.; Styring, P.; Wragg, M. S.; Maitlis, P. M. *Polyhedron* **1988**, *7*, 1861. (b) Bhatt, J.; Fung, B. M.; Nicholas, K. M.; Poon, C. D. *J. Chem. Soc., Chem. Commun.* **1988**, 1439. (c) Bruce, D. W.; Dunmur, D. A.; Maitlis, P. M.; Styring, P.; Esteruelas, M. A.; Oro, L. A.; Ros, M. B.; Serrano, J. L.; Sola, E. *Chem. Mater.* **1989**, *1*, 479. (d) Espinet, P.; Lalinde, E.; Marcos, M.; Perez, J.; Serrano, J. L. *Organometallics* **1990**, *9*, 555. (e) Espinet, P.; Perez, J.; Marcos, M.; Ros, M. B.; Serrano, J. L.; Barbera, J.; Levelut, A. M. *Organometallics* **1990**, *9*, 2028. (f) Ohta, K.; Ema, H.; Morizumi, Y.; Watanabe, T.; Fujimoto, T.; Yamamoto, I. *Liq. Cryst.* **1990**, *8*, 311. (g) Giroud-Godquin, A. M.; Maitlis, P. M. *Angew. Chem., Int. Ed. Engl.* **1991**, *30*, 375.

(2) (a) Moore, J. S.; Stupp, S. I. *Polym. Bull.* **1988**, *19*, 251. (b) Espinet, P.; Etxebarria, J.; Marcos, M.; Perez, J.; Remon, A.; Serrano, J. L. *Angew. Chem., Int. Ed. Engl.* **1989**, *28*, 1065. (c) Serrano, J. L.; Romero, P.; Marcos, M.; Alonso, P. J. *J. Chem. Soc., Chem. Commun.* **1990**, 859. (d) Bruce, D. W.; Dunmur, D. A.; Maitlis, P. M.; Manterfield, M. M.; Orr, R. *J. Mater. Chem.* **1991**, *1*, 255.

(3) (a) Piechocki, C.; Simon, J.; Skoulios, A.; Guillon, D.; Weber, P. *J. Am. Chem. Soc.* **1982**, *104*, 5245. (b) Piechocki, C.; Simon, J. *Nouv. J. Chim.* **1985**, *9*, 159. (c) Blanzat, B.; Barthou, C.; Tercier, N.; Andre, J. J.; Simon, J. *J. Am. Chem. Soc.* **1987**, *109*, 6193. (d) Sirlin, C.; Bosio, L.; Simon, J. *J. Chem. Soc., Chem. Commun.* **1987**, 379. (e) Simon, J.; Sirlin, C. *Pure Appl. Chem.* **1989**, *61*, 1265. (f) Belarbi, Z.; Sirlin, C.; Simon, J.; Andre, J. J. *J. Phys. Chem.* **1989**, *93*, 8105.

(4) Van der Pol, J. F.; Neeleman, E.; Zwikker, J. W.; Nolte, R. J. M.; Drenth, W.; Aerts, J.; Visser, R.; Picken, S. J. *Liq. Cryst.* **1989**, *6*, 577.

(5) (a) Gregg, B. A.; Fox, M. A.; Bard, A. J. *J. Chem. Soc., Chem. Commun.* **1987**, 1134. (b) Gregg, B. A.; Fox, M. A.; Bard, A. J. *J. Am. Chem. Soc.* **1989**, *111*, 3024.

(6) Esteruelas, M. A.; Oro, L. A.; Sola, E.; Ros, M. B.; Serrano, J. L. *J. Chem. Soc., Chem. Commun.* **1989**, 55.

(7) Esteruelas, M. A.; Sola, E.; Oro, L. A.; Ros, M. B.; Marcos, M.; Serrano, J. L. *J. Organomet. Chem.* **1990**, *387*, 103.

(8) Marcos, M.; Ros, M. B.; Serrano, J. L.; Esteruelas, M. A.; Sola, E.; Oro, L. A.; Barbera, J. *Chem. Mater.* **1990**, *2*, 748.

[†] Universidad de Zaragoza-CSIC.
[‡] Université Paris-Sud.

0020-1669/92/1331-0732$03.00/0 © 1992 American Chemical Society

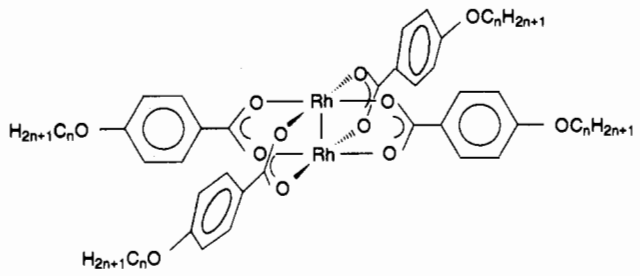

Figure 1.

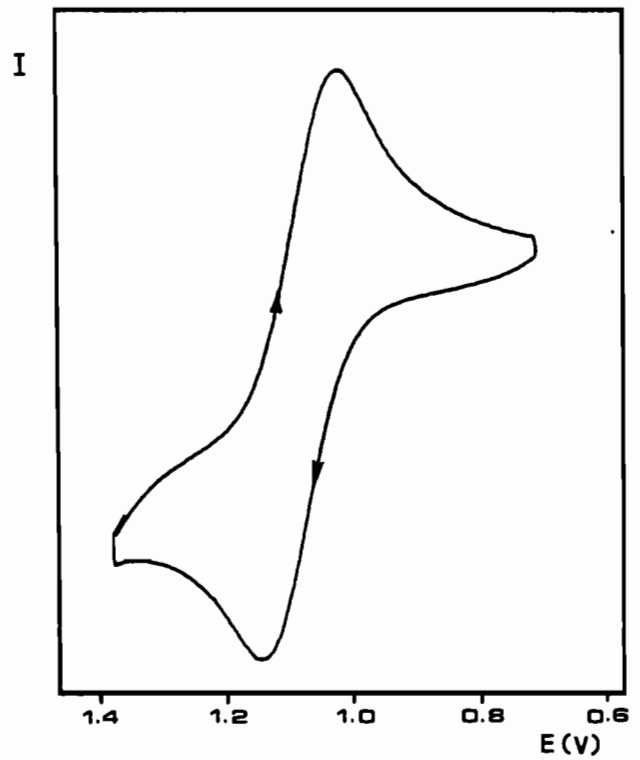

Figure 2. Cyclic voltammogram for the oxidation process of $[Rh_2(\mu\text{-}O_2CC_6H_4\text{-}4\text{-}OC_{12}H_{25})_4]$ (**5**), in CH_2Cl_2/CH_3CN (10/1).

the $(OCO)_{asym}$, $(OCO)_{sym}$, and (O–C) stretching modes at 1551, 1391, and 1250 cm^{-1}, irrespective of the alkyloxy chain length. The value of $\nu(OCO)_{asym}$ absorption shows a displacement of about 130 cm^{-1} in relation to the same absorption of the free acid. The displacement, together with the value found for $\Delta\nu(OCO) = \nu(OCO)_{asym} - \nu(OCO)_{sym} = 160$ cm^{-1}, agrees with a bridging

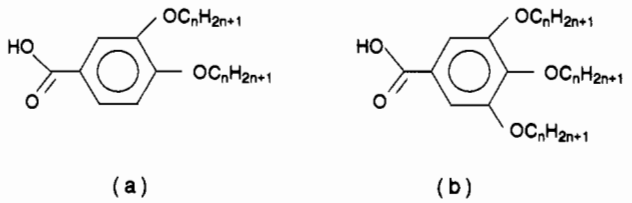

Figure 3.

coordination of the benzoate ligands.[17] Additionally, the IR spectra show two bands at 380 and 505 cm^{-1}, which can be assigned to the $\nu(Rh\text{–}O)_{asym}$ and $\nu(Rh\text{–}O)_{sym}$ modes, respectively.

The ^1H NMR spectra confirm the equivalence of the four benzoate ligands, in accordance with the proposed structure (Figure 1). However, the aromatic proton signals are broad, and no coupling constants can be obtained. This broadness can be attributed to the existence of small amounts of coordinating solvents or to the presence of paramagnetic impurities.[18]

Complexes **1**–**7** have been electrochemically characterized. A typical cyclic voltammogram for the oxidation process is shown in Figure 2, and half-wave potentials ($E_{1/2}$) for the oxidations under various solution conditions are listed in Table I. In all cases oxidation produces a single peak on the forward scan and a coupled reduction peak on the backward sweep. The ratio of cathodic to anodic peak current was close to unity at all scan rates, consistent with the absence of coupled chemical reactions. Potential separation between the cathodic and anodic peak potentials (ΔE_p) varied in the different solvents and increased with sweep rate. All these data are in good agreement with diffusion-controlled one-electron-transfer processes.

Similar oxidation processes have been reported for other dinuclear rhodium(II) complexes containing carboxylates as ligands.[19] The values of $E_{1/2}$ found for complexes **1**–**7** are consistent with those obtained for similar compounds.[18,20,21] These values do not show substantial variations under the different solvent conditions, in spite of the fact that in coordinating solvents (S) the major species are the diadducts $[Rh_2(\mu\text{-}O_2CC_6H_4\text{-}4\text{-}OC_nH_{2n+1})_4(S)_2]$, as can be inferred from the different colors of the solutions.

The electrochemical oxidation of the complex $[Rh_2(\mu\text{-}O_2CCH_3)_4]$ leads to the cationic species $[Rh_2(\mu\text{-}O_2CCH_3)_4]^+$, which retains the dinuclear structure of the starting complex.[22] Nevertheless, we failed to prepare salts of the analogous cations $[Rh_2(\mu\text{-}O_2CC_6H_4\text{-}4\text{-}OC_nH_{2n+1})_4]^+$ by chemical oxidation of complexes **1**–**7**, probably due to the high value of the oxidation potential.

The dinuclear complexes $[Rh_2(\mu\text{-}O_2CR)_4]$ form adducts with a great variety of ligands.[23] In such adducts the incoming ligands coordinate trans to the Rh–Rh bond. Similarly, our complexes react with ligands such as CO or pyrazine to give diadduct compounds. Thus, the reaction of CO with complex **3** yields the dicarbonyl adduct $[Rh_2(\mu\text{-}O_2CC_6H_4\text{-}4\text{-}OC_{10}H_{21})_4(CO)_2]$ (**8**), which shows a sharp $\nu(CO)$ absorption at 2095 cm^{-1} in the Nujol IR spectrum. However, complex **8** is only stable under a CO atmosphere and reverts to the starting material under Ar, precluding the complete characterization of the compound. Similar behavior has been reported for the parent complex $[Rh_2(\mu\text{–}$

(9) Sola, E. Ph.D. Thesis, University of Zaragoza, 1991.
(10) (a) Giroud-Godquin, A. M.; Sigaud, G.; Achard, M. F.; Hardouin, F. *J. Phys. Lett. (Paris)* **1984**, *45*, L387. (b) Giroud-Godquin, A. M.; Gaulthier, M. M.; Sigaud, G.; Hardouin, F.; Achard, M. F. *Mol. Cryst. Liq. Cryst.* **1986**, *132*, 35.
(11) Cayton, R. H.; Chisholm, M. H.; Darrington, F. D. *Angew. Chem., Int. Ed. Engl.* **1990**, *29*, 1481.
(12) (a) Maldivi, P.; Giroud-Godquin, A. M.; Marchon, J. C.; Guillon, D.; Skoulios, A.; Strommen, D. P. *Chem. Phys. Lett.* **1989**, *157*, 552. (b) Marchon, J. C.; Maldivi, P.; Giroud-Godquin, A. M.; Guillon, D.; Skoulios, A.; Stromen, D. P. *Philos. Trans. R. Soc. London* **1990**, *A330*, 109.
(13) (a) Giroud-Godquin, A. M.; Marchon, J. C.; Guillon, D.; Skoulios, A. *J. Phys. Chem.* **1986**, *90*, 5502. (b) Poizat, O.; Stromen, D. P.; Maldivi, P.; Giroud-Godquin, A. M.; Marchon, J. C. *Inorg. Chem.* **1990**, *29*, 4853.
(14) (a) Giroud-Godquin, A. M.; Marchon, J. C.; Guillon, D.; Skoulios, A. *J. Phys. Lett (Paris)* **1984**, *45*, L681. (b) Giroud-Godquin, A. M.; Latour, J. M.; Marchon, J. C. *Inorg. Chem.* **1985**, *24*, 4454. (c) Abied, H.; Guillon, D.; Skoulios, A.; Weber, P.; Giroud-Godquin, A. M.; Marchon, J. C. *Liq. Cryst.* **1987**, *2*, 269.
(15) Cook, M. J.; Daniel, M. F.; Harrison, K. J.; McKeown, N. B.; Thomson, A. J. *J. Chem. Soc., Chem. Commun.* **1987**, 1086.
(16) Ohta, K.; Watanabe, T.; Fujimoto, T.; Yamamoto, I. *J. Chem. Soc., Chem. Commun.* **1989**, 1611.
(17) Deacon, G. B.; Phillipps, R. J. *Coord. Chem. Rev.* **1980**, *33*, 227.
(18) Das, K.; Kadish, K. M.; Bear, J. L. *Inorg. Chem.* **1978**, *17*, 930.
(19) (a) Chen, S. J.; Dunbar, K. R. *Inorg. Chem.* **1990**, *29*, 588. (b) Zhu, T. P.; Ashan, M. Q.; Malinski, T.; Kadish, K. M.; Bear, J. L. *Inorg. Chem.* **1984**, *23*, 3. (c) Chavan, M. Y.; Zhu, T. P.; Lin, X. Q.; Ashan, M. Q.; Bear, J. L.; Kadish, K. M. *Inorg. Chem.* **1984**, *23*, 4538. (d) Chakravarty, A. R.; Cotton, F. A.; Tocher, D. A.; Tocher, J. H. *Organometallics* **1985**, *4*, 8.
(20) Wilson, C. R.; Taube, H. *Inorg. Chem.* **1975**, *14*, 2276.
(21) Drago, R. S.; Tanner, S. P.; Richman, R. M.; Long, J. R. *J. Am. Chem. Soc.* **1979**, *101*, 2897.
(22) (a) Ziolkowski, J. J.; Mosaner, M.; Gloniak, T. *J. Chem. Soc., Chem. Commun.* **1977**, 760. (b) Cannon, R. D.; Powell, D. B.; Sarawek, K.; Stillman, J. S. *J. Chem. Soc., Chem. Commun.* **1976**, 31.
(23) Boyar, E. B.; Robinson, S. D. *Coord. Chem. Rev.* **1983**, *50*, 109.

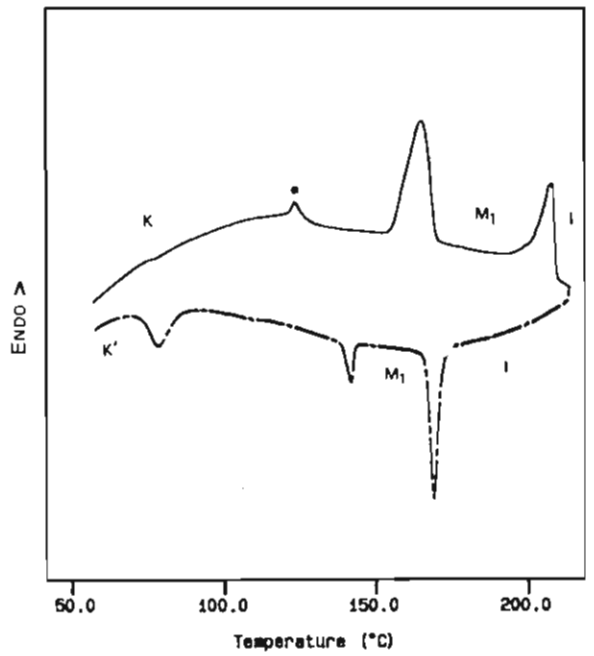

Figure 4. DSC thermogram of the first heating and cooling processes of complex **3**. An asterisk indicates the peak due to the endothermic loss of small amounts of coordinated water.

$O_2CCH_3)_4(CO)_2]$.[18] The use of N-donor ligands usually leads to more stable diadduct complexes.[23] Thus, the treatment of a hexane suspension of **1** with pyrazine, in molar ratio 1/2 or in excess of pyrazine, led to the formation of a red solid. The elemental analysis of this solid agrees with the stoichiometry $[Rh_2(\mu\text{-}O_2CC_6H_4\text{-}4\text{-}OC_8H_{17})_4(N_2C_4H_4)]_n$ (**9**), showing that, even in an excess of pyrazine, the resulting complex contains only one molecule of the bidentate ligand per molecule of dimer. The ^1H NMR spectrum of complex **9** shows the resonances expected for the carboxylates ligands together with a singlet corresponding to the four pyrazine protons, suggesting the formation of polymeric species. Similar pyrazine compounds, obtained from isostructural copper(II) complexes, have been formulated as oligomeric/polymeric species.[24]

The complexes $[Rh_2(\mu\text{-}O_2CC_6H_3\text{-}3,4\text{-}(OC_{10}H_{21})_2)_4]$ (**10**) and $[Rh_2(\mu\text{-}O_2CC_6H_2\text{-}3,4,5\text{-}(OC_{10}H_{21})_3)_4]$ (**11**) were obtained as waxy green materials following a synthetic procedure essentially similar to that employed for complexes **1–7** but starting from the benzoic acids shown in Figure 3a,b,respectively. The microanalysis obtained demonstrate the proposed stoichiometry whereas the ^1H NMR spectra confirm the equivalence of the four benzoate groups, in accordance with the dinuclear structure typical of these Rh(II) complexes.

Mesogenic Properties. The complexes $[Rh_2(\mu\text{-}O_2CC_6H_3\text{-}4\text{-}OC_nH_{2n+1})_4]$ display mesogenic properties from $n = 10$ and up. Figure 4 shows the first DSC scan for complex **3**. The heating scan show two endothermic peaks: The first, at 156 °C, corresponds to the transition between the crystalline phase and a viscous mesophase M_1. The second, at 203 °C, is due to the clearing of the M_1 mesophase into the isotropic liquid. The cooling DSC trace contains the peak corresponding to the isotropic liquid to M_1 transition, but instead of the exothermic M_1 to crystal transition it shows two new lower energy transitions.

Figure 5a shows the mosaic texture of the mesophase M_1 obtained by cooling the isotropic liquid phase. The two exothermic low-energy transitions observed by DSC do not affect this mosaic texture, which remains unchanged up to room temperature. However, at this temperature, the sample is solid, as can be confirmed by mechanical stress. In subsequent heating and cooling cycles only the peaks present in the cooling scan are obtained. This behavior suggests that after a heating and cooling cycle the material crystallizes into a solid phase different from the starting crystal phase. After several weeks, the sample shows the same DSC trace obtained in the first thermal cycle, which indicates the slow transformation of this final crystal phase into the crystalline phase present before any thermal cycle.

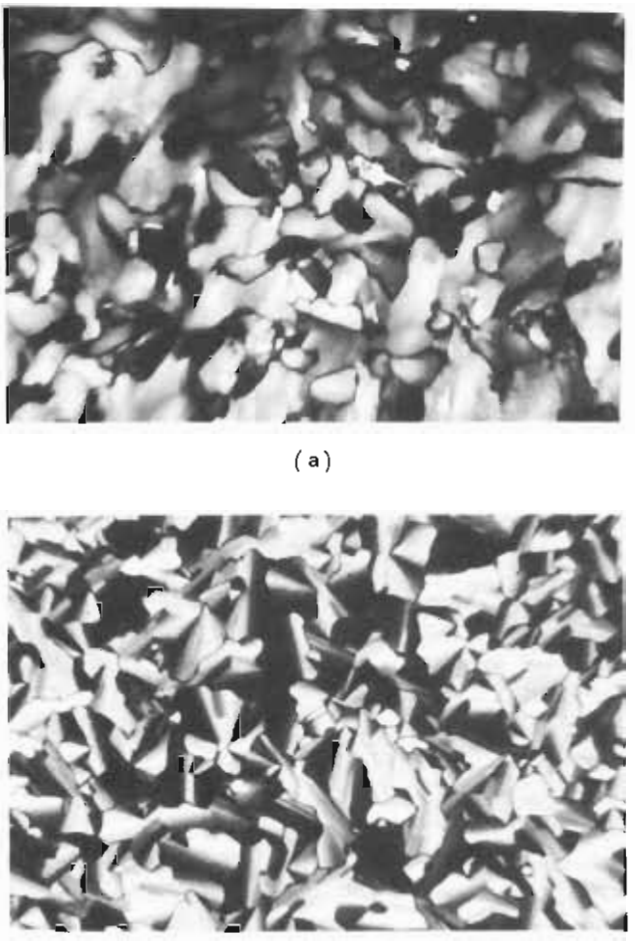

Figure 5. Optical texture (crossed polarizers) of (a) $[Rh_2(\mu\text{-}O_2CC_6H_4\text{-}4\text{-}OC_{11}H_{23})_4]$ (**4**) in the mesophase M_1 and (b) $[Rh_2(\mu\text{-}O_2CC_6H_2\text{-}3,4,5\text{-}(OC_{10}H_{21})_3)_4]$ (**11**) in the mesophase M_2.

Table II. Temperatures and Enthalpies for the Phase Transitions of $[Rh_2(\mu\text{-}O_2CC_6H_4\text{-}4\text{-}OC_nH_{2n+1})_4]$ Complexes

complex	n	transition	temp/°C	ΔH/J g^{-1}
1	8	C-I	230.8	56.3
2	9	C-I	206.5	42.9
3	10	C-M_1	156.1	25.7
		M_1-I	203.0	14.7
4	11	C-M_1	142.7	20.5
		M_1-I	203.7	14.2
5	12	C-C′	94.5	10.9
		C′-M_1	113.2	17.9
		M_1-I	204.9	18.9
6	13	C-M_1	103.3	20.0
		M_1-I	201.8	23.9
7	14	C-M_1	94.0	13.7
		M_1-I	189.0	17.9

The other mesogenic members of this series (complexes **4–7**) show a thermal behavior similar to that described for **3**. Table II collects the temperatures and enthalpy data for the phase transitions obtained, and Figure 6 represents the DSC thermograms of the first heating and cooling processes for complexes **1–7**.

As can be observed, all the complexes show similar isotropization temperatures, whereas the mesogenic ranges widen as the length of the alkyloxy chain increases. The supercooling phenomena obtained for the M_1 to isotropic transitions remain even

(24) Attard, G. S.; Cullum, P. R. *Liq. Cryst.* **1990**, *8*, 299.

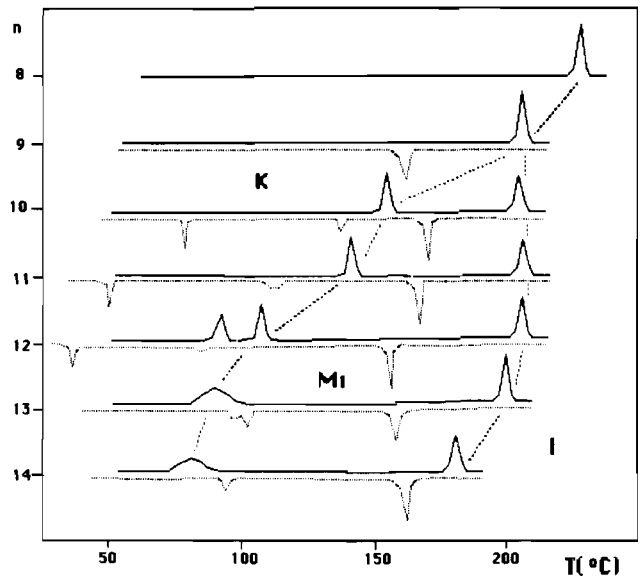

Figure 6. Schematic representation of the DSC thermograms of $[Rh_2(O_2CC_6H_4\text{-}4\text{-}OC_nH_{2n+1})_4]$ complexes.

at very slow scanning rates. The complexes show good thermal stabilities, starting to decompose at temperatures above 240 °C.

Complex **9** does not show mesogenic properties, decomposing in the solid state at about 160 °C. The same behavior has been found for some other long chain carboxylate copper(II) complexes with pyrazine ligands.[24]

Complex **10** shows a viscous fluid phase at room temperature with a mosaic texture. On heating (137.8 °C, ΔH = 9.1 J g^{-1}), this phase transforms into a new mesophase M_2. During the phase transition the texture of the low-temperature phase becomes progressively darker, leading to a homeotropic texture which is stable in an interval of about 2 °C. This homeotropic texture gives rise to a pseudo-focal-conic texture that characterizes the mesophase M_2. This transition is reproducible in the cooling process. The mesophase M_2 is stable until the clearing point (235 °C), the temperature at which the complex starts to decompose. Due to decomposition, the M_2 to isotropic transition cannot be clearly observed in the DSC thermogram.

Complex **11** also displays liquid-crystal behavior. At room temperature it shows a very viscous phase which slowly transforms into a more fluid mesophase as the temperature is raised. This transition produces a wide peak in the DSC thermogram, centered at 115 °C, in accordance with the slowness of the transition. The high-temperature phase is stable until the clearing point (202 °C, ΔH = 7.4 J g^{-1}) and shows textures similar to those found for M_2. Figure 5b shows the pseudo-focal-conic texture obtained for the M_2 mesophase of complex **11** on cooling from the isotropic liquid.

Table III. X-ray Diffraction Data for the M_1 Mesophase of Complex **3** at 170 °C[a]

d_{obs}/Å	d_{calc}/Å	*hkl*	d_{obs}/Å	d_{calc}/Å	*hkl*
27.58	27.53	200	6.74	6.74	710
13.74	13.77	400	6.55	6.53	020
12.70	12.70	110	6.36	6.36	220
10.64	10.64	310	5.53	5.54	910
9.20	9.18	600	4.86	4.86	001
8.42	8.41	510	4.33	4.34	130
6.87	6.88	800	4.04	4.04	530

[a] a = 55.05 Å, b = 13.06 Å, and c = 4.86 Å.

Table IV. Lattice Parameters (Å) for the High-Temperature Phase (M_1) of $[Rh_2(\mu\text{-}O_2CC_6H_4\text{-}4\text{-}OC_nH_{2n+1})_4]$ Complexes

complex	*n*	*a*	*b*	*c*	temp/°C
3	10	55.05	13.06	4.86	170
4	11	58.05	13.09	4.86	160
5	12	61.63	13.09	4.82	153
6	13	63.90	13.31	4.91	118

Structures of the Phases. In order to clarify the mesomorphism of these compounds, we performed an X-ray structural study. In a first step, we obtained powder patterns of the samples at various temperatures.

For complex **3** three different patterns were obtained: at 170 °C, at 20 °C after a heating cycle, and at 20 °C before any heating cycle. The high-temperature-phase (M_1) pattern (Table III) corresponds to an orthorhombic lattice of parameters: a = 55.05 Å, b = 13.06 Å, and c = 4.86 Å. All the reflections (if one excepts 001) correspond to l = 0, h or $k \neq 0$ and $h + k = 2n$, which indicates a two-dimensional centered rectangular lattice lying on the *ab* plane (space group *Cmmm*).

On cooling of the sample to 20 °C, parameter a is shorter and the lattice is still orthorhombic with a = 49.30 Å, b = 12.96 Å, and c = 4.86 Å. However, the 3D crystalline character can be deduced from the existence of the 301 reflection. Moreover, the presence of this reflection excludes the possibility of a *C*-centered face. The space group is probably *Pbmn*. This implies that the molecules are tilted in relation to the column axis (Figure 7a) in the *ac* plane, which is also consistent with the shortening of parameter a.

The pattern obtained for the crystalline phase present before any heating cycle corresponds to a 3D orthorhombic lattice of parameters a = 23.50 Å, b = 13.19 Å, and c = 4.82 Å (space group *Pmmm*). This pattern is not recovered after a thermal cycle going up to 170 °C.

Complexes **4–6** have been studied in their high-temperature phase. The lattice is also a *C*-centered orthorhombic lattice with a two-dimensional character. The two lattice constants b and c are nearly independent of the compound, while a increases with the chain length (3 Å/carbon atom) (see Table IV). In order to confirm the mesogenic character of the high-temperature phase,

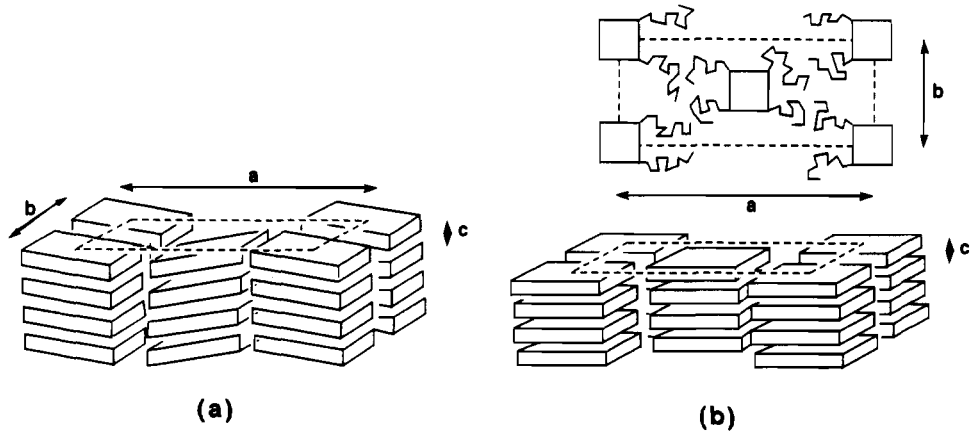

Figure 7. (a) Schematic representation of the crystalline phase shown by complex **3**, after a heating cycle. (b) Schematic representation of the proposed structure for the mesophase M_1.

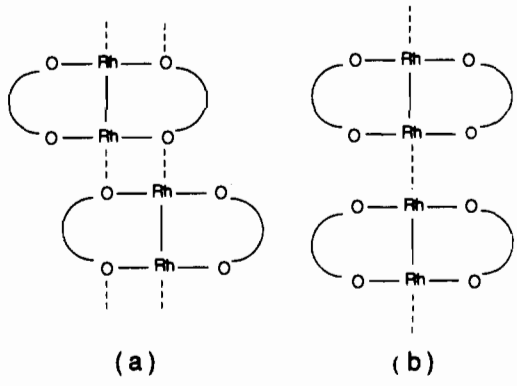

Figure 8.

we aligned the samples in thin mica sheets with a spatula. The *c* direction was parallel to the stretching direction, and *a* was more or less perpendicular to the mica sheet. It is worth mentioning that the absence of *hkl* reflections with *h* or *k* and $l \neq 0$ can fit a lamellar structure, with a layer thickness $c = 4.86$ Å (for complex **3**), or a columnar structure, with a mean periodicity in a column of 4.86 Å. In the first case, the *hk*0 reflections must extend out of the equatorial plane with a length of about 1/4.86 Å, while in the latter case the 001 reflection will have a rectangular shape 1/13 Å × 1/55 Å. Since we did not obtain a good alignment, we cannot distinguish between these two possibilities from the aligned patterns. However, the width of the rings in powder pattern in consistent with a columnar phase. Each column is made of single complexes regularly spaced at distances of 4.86 Å.

This stacking periodicity is similar to that found for the columnar mesophases of some dinuclear rhodium complexes,[13] where the molecules stack with their Rh–Rh direction parallel to the column axis. The distance 4.86 Å is only slightly longer than that expected for two Rh–Rh bonds (2.38 Å in rhodium(II) acetate[23]). X-ray and EXAFS studies performed for the columnar mesophase of dinuclear rhodium and copper complexes[12,25] with alkanoate ligands show a zigzag arrangement of the dimers within the columns. In these systems the periodicities measured correspond to the sum of the M–M bond distance and the distance of intermolecular M···O contacts. This organization (Figure 8a) allows better packing of the molecules, leading to stacking distances shorter than those possible for a hypothetical Rh–Rh···Rh–Rh linear arrangement (Figure 8b).

For our complexes option a seems more likely in the view of the measured periodicities *c*, since option b would force the dimers to approach each other at Rh–Rh bonding distances. Accordingly, recent research into mesogenic dinuclear carboxylate complexes of Cr and Mo also suggests that in the mesophase the axial M···O interactions are maintained.[11]

The dinuclear cores of the molecules are located in the apex and in the center of the two-dimensional lattice. The chain organization can be estimated from an analysis of the mean area per chain. Since $a \gg b$ and *c*, and *a* increases with the chain length, *b* and *c* being practically constant, the chains are elongated along *a* and in an area $b \times c$ (of about 63 Å for complex **3**). In this area it is possible to have either have four chains in an interdigitate configuration or two if the chains of two different molecules are only in contact by their methyl terminal end group. The latter hypothesis is the only one consistent with the minimum chain area (19 Å^2)[14] and corresponds to a mean area of 31.5 Å^2. In such a case, each molecule occupies a length $a/2$ of 27.5 Å for complex **3**. It is known that, at a given temperature, the volume filled by a methylene group has a constant value, independent of the type of mesophase and chain length.[26] Assuming a volume of 28 Å^3/CH$_2$ at 170 °C, the chain length should be of 17.5 Å and the core length 10 Å. The last value is slightly smaller than that calculated by using Dreiding models (11.5 Å). This difference may be due to a partial interpenetration of the rigid and flexible parts, provided that the free space between the aromatic rings can be partially filled by the chains. Figure 7b shows a schematic representation of the structure proposed for M_1. The density calculated for this structure is of 1.2 g cm^{-3}.

The powder patterns of the high-temperature phase M_2 of complexes **10** and **11** are characteristic of a columnar mesophase with a two-dimensional hexagonal lattice (space group *P6/mmm*). The intercolumnar distances obtained are 29.1 Å for **10** and 26.6 Å for **11**. A narrow reflection in the wide-angle X-ray region corresponding to the order of the intermolecular distance within the columns is absent, and so, phase M_2 is a disordered hexagonal columnar mesophase. The shortening of the intercolumnar distance for **11** in relation to that obtained for **10** must be related to an increase in the mean intracolumnar distance. This observation is consistent with the greater spatial requirements of the chains out of the molecular plane for complex **11**.

The patterns of the low-temperature phases of complexes **10** and **11** are not definitive for the unambiguous characterization of these phases. For complex **10** the powder pattern of the room temperature phase is consistent with the existence of a *C*-centered orthorhombic lattice; $a = 45.7$ Å and $b = 30.1$ Å. The diffraction pattern obtained does not allow us to distinguish clearly between a rectangular mesophase and a 3D solid. However, the small number of diffraction rings suggests that the phase is a mesophase rather than a more ordered 3D phase. The assignment of this phase to a rectangular columnar mesophase, similar to M_1, also agrees with the observed mosaic texture, the fluidity of the phase, and the previously mentioned characteristics of the phase transition into the high-temperature mesophase M_2.

The diffraction pattern obtained for the room-temperature phase of complex **11** corresponds to a 3D monoclinic phase of parameters: $a = 33.28$ Å, $b = 20.38$ Å, $c = 10.10$ Å, and $\gamma = 113.3°$. This structure gives a density of 1.24 g cm^{-3} with $Z = 2$. However, since there are few rings with $l \neq 0$, the indexation of this pattern is not completely evident. This uncertainty with regard to the lattice assignment may be due to imperfect organization of the crystal phase, which may also account for the waxy appearance of the material at room temperature.

Discussion

Rectangular columnar mesophases have been obtained in some organic derivatives with flat truxene or triphenylene cores and six (alkyloxy)benzoyl chains[27] and more recently in a series of bi-swallow-tailed polycatenar compounds.[28] Additionally, a rectangular columnar mesophase, characterized by X-ray diffraction, has been reported for a macrocyclic copper(II) complex.[16] All these compounds display mesophases in which the molecules are disordered along the long axes of the columns, whereas the mesophase shown by complexes **3–7** exhibits long-range order within the columns. To the best of our knowledge, complexes **3–7** are the only materials that show an ordered rectangular columnar mesophase.

Rhodium(II) complexes with four long-chain alkanoate ligands, isostructural to complexes **3–7**, show a hexagonal columnar mesophase.[13] In this mesophase the columns have a cylindrical symmetry, consisting of a cylindrical core, formed from the rigid central groups, radially surrounded by the flexible chains. In complexes **3–7** the greater size of the rigid core in relation to the alkanoato complexes precludes the formation of the hexagonal mesophase with four paraffinic chains, which are not enough to fill the space generated by the rigid core which would ensure a cylindrical symmetry. Instead of that, the four chains tend to align

(25) (a) Abied, H.; Guillon, D.; Skoulios, A.; Dexpert, H.; Giroud-Godquin, A. M.; Marchon, J. C. *J. Phys.* (*Les Ulis, Fr.*) **1988**, *49*, 345. (b) Maldivi, P.; Guillon, D.; Giroud-Godquin, A. M.; Marchon, J. C.; Abied, H.; Dexpert, H.; Skoulios, A. *J. Chim. Phys.* (*Paris*) **1989**, *86*, 1651.

(26) Guillon, D.; Skoulios, A.; Benattar, J. J. *J. Phys.* (*Les Ulis, Fr.*) **1986**, *47*, 133.

(27) (a) Levelut, A. M. *J. Chim. Phys.* (*Paris*) **1983**, *80*, 149 and references therein. (b) Destrade, C.; Foucher, P.; Gasparoux, H.; Huu Tinh, N.; Levelut, A. M.; Malthete, J. *Mol. Cryst. Liq. Cryst.* **1984**, *106*, 121 and references therein.

(28) Diele, S.; Ziebarth, K.; Pelzl, G.; Demus, D.; Weissflog, W. *Liq. Cryst.* **1990**, *8*, 211.

Table V. Elemental Analyses and Yields for the Complexes 1-7

complex	n	anal.: found (calcd) c/%	H/%	yield/%
1	8	59.87 (59.69)	7.41 (7.34)	68
2	9	61.61 (61.04)	7.79 (7.36)	68
3	10	61.81 (61.90)	8.17 (7.64)	47
4	11	62.86 (63.05)	8.18 (7.93)	81
5	12	64.11 (63.94)	8.64 (8.19)	75
6	13	64.63 (64.76)	8.63 (8.42)	46
7	14	65.28 (65.52)	8.96 (8.64)	69

in one direction, giving rise to a rectangular columnar mesophase. On the other hand, with the same rigid core, the hexagonal mesophase can be stabilized by 12 chains, as in complex **11**.

For the derivative with eight paraffinic chains, complex **10**, the results obtained point to an intermediate situation. At low temperatures the stable phase seems to be a rectangular columnar mesophase, similar to that found in the four-chained complexes (**3**–**7**). The conformational disorder of the chains increases as the temperature is raised, allowing a better filling of the space around the rigid core. Thus, at 137 °C, the rectangular mesophase undergoes a phase transition into the hexagonal mesophase stable at high temperatures.

The results confirm that for these disklike compounds, the factor that determines the symmetry of the mesophase obtained is the relationship between the volume of the rigid core and the volume filled by the flexible substituents of the molecules.

Experimental Section

Measurements. Elemental analysis was performed with a Perkin-Elmer 240B microanalyzer. Infrared spectra were recorded on a Perkin-Elmer 783 spectrometer. ^{1}H NMR spectra were recorded on a Varian XL 200 spectrometer.

The textures of the mesophases were studied with a Meiji polarizing microscope equipped with a Mettler FP82 hot stage and FP80 central processor. Transition temperatures and enthalpies were measured by differential scanning calorimetry with a Perkin-Elmer DSC7 instrument operated at a scanning rate of 5 K min^{-1}. The apparatus was calibrated with indium (429.6 K, 28.4 J g^{-1}) as a standard.

Electrochemical measurements were made with an Inelecsa Model PDC10 potentiostat system linked to a plotter. A three-electrode cell configuration was employed consisting of platinum-wire working and auxiliary electrodes and a saturated calomel electrode (SCE). All potentials are referenced versus SCE. The solvents 1,2-dichloroethane, tetrahydrofuran, and acetonitrile were reagent grade quality and were dried by the usual procedures and distilled under argon prior to use. The supporting electrolyte was 0.1 M tetrabutylammonium hexafluorophosphate. All voltammetric measurements were made under a dry argon atmosphere.

X-ray diffraction experiments on the powder samples were made with a classical Guinier camera. A linearly collimated X-ray beam of wavelength λ = 1.5405 Å (Cu Kα_1) was obtained by reflection on a quartz monochromator. The sample was held in a Lindemann capillary (ϕ = 0.5 mm) and heated by an air stream. The temperature was held constant within 2 deg. The X-ray data were refined by a least-squares fit.

Materials. $[Rh_2(\mu\text{-}O_2CCH_3)_4]$,[29] 4-(alkyloxy)benzoates,[30] 3,4-bis(decyloxy)benzoate, and 2,3,4-tris(decyloxy)benzoate[31] were prepared by published methods. All other reagents were purchased from normal commerical suppliers. Solvent used were distilled and dried prior to use.

Preparation of $[Rh_2(\mu\text{-}O_2CC_6H_4\text{-}4\text{-}OC_nH_{2n+1})_4]$ Complexes 1-7. A mixture of $[Rh_2(\mu\text{-}O_2CCH_3)_4]$ (0.75 mmol) and the 4-(alkyloxy)benzoate (5 mmol) was placed in an evacuated 50-cm^3 round-bottomed flask. The mixture was heated at 170 °C and magnetically stirred for 2 h. Most of the excess ligand was removed by filtration after treatment of the reaction mixture with 5 mL of 1,2-dichloroethane. The resulting green solution was concentrated under reduced pressure to about 1 mL and methanol added, to yield the blue methanol adduct of the desired complex. The solid was filtered off and the coordinated methanol removed by heating at 70 °C under vacuum over 6 h; during this period the color changed from blue to light green. Microanalysis and yields of the complexes **1**-**7** are given in Table V. ^{1}H NMR ($CDCl_3$) (all complexes show similar patterns): δ 7.92, 6.70 (16 H, $O_2CC_6H_4$), 3.88 (8 H, $-OCH_2-$), 1.70 (8 H, $-OCH_2CH_2-$), 1.23 ($2n$ - 6 H), 0.85 (12 H, $-CH_3$).

Preparation of $[Rh_2(\mu\text{-}O_2CC_6H_4\text{-}4\text{-}OC_{10}H_{21})_4(CO)_2]$ (8). Bubbling of CO through a suspension of **3** (100 mg, 0.8 mmol) in 10 mL of hexane during 10 min led to the formation of a red precipitate. This solid recovered the green color of the starting complex when the CO atmosphere was replaced by Ar. IR (Nujol): ν(CO) 2095 cm^{-1}. IR (CH_2Cl_2): ν(CO) 2095 cm^{-1}.

Preparation of $[Rh_2(\mu\text{-}O_2CC_6H_4\text{-}4\text{-}OC_8H_{17})_4(N_2C_4H_4)]_n$ (9). A suspension of **1** (100 mg, 0.8 mmol) in 10 mL of hexane was treated with pyrazine (13.3 mg, 0.17 mmol). The mixture was stirred for 30 min under Ar at room temperature. The red solid obtained was filtered off, washed with hexane, and dried in vacuo. Yield: 90 mg (85%). Anal. Found: C, 59.62; H, 7.32; N, 2.40. Calcd for $C_{64}H_{88}N_2O_{12}Rh_2$: C, 59.90; H, 6.91; N, 2.18. IR (Nujol): $\nu(OCO)_{asym}$ 1610 cm^{-1}; $\nu(OCO)_{sym}$ 1395 cm^{-1}; ν(O–C) 1250 cm^{-1}. ^{1}H NMR ($CDCl_3$): δ 10.24 (s, 4 H, $N_2C_4H_4$), 8.15, 6.86 (16 H, $O_2CC_6H_4$), 3.99 (8 H, $-OCH_2-$), 1.8 (8 H, $-OCH_2CH_2-$), 1.3 (40 H), 0.87 (12 H, $-CH_3$).

Preparation of $[Rh_2(\mu\text{-}O_2CC_6H_3\text{-}3,4\text{-}(OC_{10}H_{21})_2)_4]$ (10). A mixture of $[Rh_2(\mu\text{-}O_2CCH_3)_4]$ (200 mg, 0.45 mmol) and $HO_2CC_6H_3$-3,4-$(OC_{10}H_{21})_2$ (900 mg, 2.1 mmol) was placed in an evacuated 50-cm^3 round-bottomed flask. The mixture was heated at 170 °C and magnetically stirred for 2 h. The green residue obtained was treated with 5 mL of cold hexane, and the excess ligand was removed by filtration. The resulting solution was concentrated under reduced pressure to about 1 mL and acetone added to yield a blue solid. The solid was filtered off, washed with acetone, and dried by heating at 60 °C under vacuum over 48 h. Anal. Found: C, 66.72; H, 10.08. Calcd for $C_{108}H_{180}O_{16}Rh_2$: C, 66.71; H, 9.33. ^{1}H NMR ($CDCl_3$): δ 7.58 (d, 4 H, J = 8.4 Hz), 7.50 (s, 4 H), 6.68 (d, 4 H, J = 8.4 Hz), 3.90 (16 H, m, $-OCH_2-$), 1.8–1.2 (br, 64 H), 0.87 (24 H, m, $-CH_3$).

Preparation of $[Rh_2(\mu\text{-}O_2CC_6H_2\text{-}3,4,5\text{-}(OC_{10}H_{21})_3)_4]$ (11). A mixture of $[Rh_2(\mu\text{-}O_2CCH_3)_4]$ (200 mg, 0.45 mmol) and $HO_2CC_6H_2$-3,4,5-$(OC_{10}H_{21})_3$ (1100 mg, 1.8 mmol) was placed in an evacuated 50-cm^3 round-bottomed flask. The mixture was heated at 170 °C and magnetically stirred for 2 h. The green residue obtained was dissolved in CH_2Cl_2 and separated from the excess ligand by column chromatography, using CH_2Cl_2 as an eluent. The green fraction obtained was dried and treated with acetone to yield a blue solid. The solid was filtered off, washed with acetone, and dried by heating at 60 °C under vacuum over 48 h. Anal. Found: C, 69.74; H, 11.30. Calcd for $C_{148}H_{260}O_{20}Rh_2$: C, 69.29; H, 10.21. ^{1}H NMR ($CDCl_3$): δ 7.26 (s, 4 H, $-C_6H_2-$), 3.83 (24 H, m, $-OCH_2-$), 1.6–1.2 (br, 192 H), 0.87 (36 H, m, $-CH_3$).

Registry No. **1**, 138385-08-7; **2**, 138385-09-8; **2**$^+$, 138385-19-0; **3**, 138385-10-1; **3**$^+$, 138385-20-3; **4**, 138385-11-2; **4**$^+$, 138385-21-4; **5**, 138385-12-3; **5**$^+$, 138385-22-5; **6**, 138385-13-4; **6**$^+$, 138385-23-6; **7**, 138385-14-5; **7**$^+$, 138385-24-7; **8**, 138385-15-6; **9**, 138385-16-7; **10**, 138385-17-8; **11**, 138385-18-9; $[Rh_2(\mu\text{-}O_2CCH_3)_4]$, 15956-28-2.

(29) Rempel, G. A.; Legzdins, P.; Smith, H.; Willkinson, G. *Inorg. Synth.* **1972**, *13*, 90.
(30) Gray, G. W.; Jones, B. *J. Chem. Soc.* **1953**, 4179.
(31) Strzelecka, H.; Jallabert, C.; Veber, M.; Malthete, J. *Mol. Cryst. Liq. Cryst.* **1988**, *156*, 347.